

“Band-gap theory” of strong ferromagnetism: Application to concentrated crystalline and amorphous Fe- and Co-metalloid alloys

A. P. Malozemoff, A. R. Williams, and V. L. Moruzzi

IBM Thomas J. Watson Research Center, Yorktown Heights, New York 10598

(Received 28 July 1983)

We extend the early work of Stoner, Mott, Friedel, and Terakura and Kanamori, which relates alloy magnetization to solute valence. We describe the conditions under which the simple formula $\mu_{av} = \mu_A^0 - x(10 + Z_B - Z_A)$ can be expected to apply. In particular, we consider Fe- and Co-metalloid alloys. Here μ_{av} is the atom-averaged moment, μ_A^0 is the host moment, x is the metalloid-atom fraction, and Z_B and Z_A are the valence of metalloid and transition metal, respectively. We show that the validity of this formula rests on the existence of band gaps in the density of states in the spin-up band. Spin-polarized band-structure calculations do indeed show band gaps in moderately concentrated ($x \sim 0.25$) compounds and indicate that μ_A^0 should be somewhat higher for fcc than bcc structures. The theory compares well with data on concentrated amorphous and crystalline alloys of Co with Au, B, Sn, and P, and of Fe with Au, B, Al, Ga, and Si. Our explanation of this large amount of data is far simpler than, and as accurate as, any previous efforts at explanation.

I. INTRODUCTION

There exists a vast literature on the magnetic moments of alloys, both crystalline and amorphous, of the transition metals Fe, Co, and Ni with metalloids such as B, Al, Si, Ge, and P. Although Stoner¹ and Mott² first offered an interpretation of the Ni alloys almost 50 years ago, a correct interpretation of the Fe and Co alloys has remained a topic of lively debate ever since. Here we describe a simple interpretation which spans, not only the Ni alloys, but also many of the Co and Fe alloys, particularly the concentrated ones. Our approach is based on our band-structure calculations, coupled with the reinterpretation by Terakura and Kanamori^{3,4} of the formula of Mott⁵ and Friedel⁶ for transition-metal-metalloid alloys. We have previously given a general introduction to this approach.^{7,8} Here we concentrate on the metal-metalloid alloys, describing more details of the theory, its historical background, and the comparison to experiment.

The most important requirement for this theory is the existence of gaps or deep minima in the density of states as a function of energy. Such band gaps have two important effects: (1) They provide a necessary condition for strong magnetism in the framework of Stoner's "collective electron ferromagnetism" theory.^{9,10} We will introduce a simple construction which helps to visualize why strong magnetism is so common when such gaps are present. (2) Gaps also give rise to an important conservation law for the integrated density of states under alloying, as first clarified by Terakura and Kanamori.^{3,4} This state-conservation law, coupled with strong magnetism, leads to a simple formula for the magnetic moment of transition-metal alloys. We will refer to this theory as the "band-gap theory."

Ironically, the predictions of the theory coincide, in some cases, with those of the original rigid-band theory,

even though there are gross errors in the basic assumptions of that earlier theory. This interrelationship has caused much confusion in the literature, which we attempt to clarify with a brief historical review.

Our contribution to the band-gap theory, as developed in this paper, is to recognize its generality and applicability to many systems previously not considered in this framework. In particular, we show, using band-structure calculations, that gaps can persist in concentrated metal-metalloid alloys, whereas previously the theory had been developed primarily for dilute alloys.^{3,4} We compare the theory to previously published experimental results on concentrated amorphous and crystalline alloys; most systems agree well. In this comparison we use a generalized Slater-Pauling construction which we have introduced recently⁸ and which helps to focus on the essential concepts of the theory.

II. STONER CRITERION FOR STRONG MAGNETISM

We begin with a review of the Stoner theory of collective electron ferromagnetism.^{9,10} We focus particularly on the relationship of the Fermi level to valleys or gaps in the paramagnetic state density. This is related to the question of why in strong magnets such as Co and Ni the top of the majority-spin d band is found, both theoretically and experimentally, to be a finite energy below the Fermi energy.

These questions can be answered using the simplest form of Stoner's theory. That is, we can assume (only for the purpose of this discussion) that the states of the paramagnetic system are shifted rigidly in energy by the exchange interaction, resulting in a transfer of electrons from the minority-spin- (down) states immediately below the paramagnetic Fermi level to majority-spin- (up) states

immediately above the paramagnetic Fermi level. The process stops when the total energy is minimized. In a strong magnet, the total energy continues to decrease as we transfer electrons to the majority-spin d band, but this conversion of spin-down electrons to spin-up electrons must, of course, stop when the spin-up d band is filled. Does the splitting stop at this point too?

Figure 1 contains a graphical construction designed to answer this question. The upper portion of Fig. 1 shows a schematic d -band state density, drawn as a rectangle; the lower portion of the figure shows the corresponding integrated state density, that is, the total number of states lying below any given energy. The conversion of spin-down electrons to spin-up electrons to create a magnetic moment is represented in the figure by values of the integrated state density that differ for spin-up and spin-down electrons by the magnetization M . Note that because any electrons added to the spin-up band must come from the spin-down band, the ferromagnetic values of the integrated state density N^\uparrow and N^\downarrow must be symmetrically displaced with respect to the paramagnetic value N^P . Thus any value of the magnetization M implies values for both N^\uparrow and N^\downarrow , and these in turn imply, via the integrat-

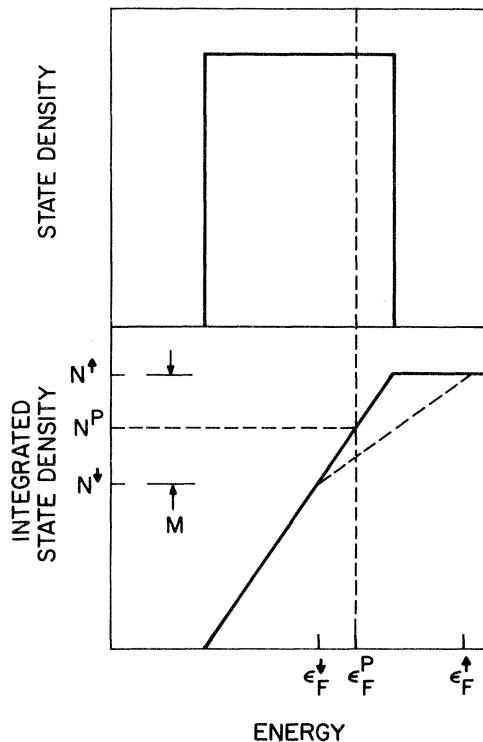


FIG. 1. State density and integrated state densities that explain why the ferromagnetic Fermi level in general lies above the top of the d band in strong ferromagnets. The upper graph shows a schematic d -band state density and the lower graph shows the corresponding integrated state density. The magnetization $M (= \mu_{av})$ is the difference between the number of spin-up and spin-down electrons. $2N^P$ is the number of electrons of either spin in the paramagnetic state and ϵ_F^P is the corresponding Fermi energy. The total energy is minimized when the magnetization causes the slope of the dashed chord $M/(\epsilon_F^\uparrow - \epsilon_F^\downarrow)$ to equal the inverse Stoner exchange integral I^{-1} .

ed state density, values for both the spin-up and spin-down Fermi energies ϵ_F^\uparrow and ϵ_F^\downarrow . (For convenience we speak here of different spin-up and spin-down Fermi energies rather than using the equivalent approach of shifting the bands relative to a single common Fermi energy.) Note that the resulting values of ϵ_F^\uparrow and ϵ_F^\downarrow are *not*, in general, symmetrically displaced, relative to the paramagnetic Fermi level ϵ_F^P . Only in the special case of a constant state density is the spin splitting symmetric with respect to ϵ_F^P .

We are now in a position to understand the particular value of the magnetization that minimizes the total energy, i.e., how far the spin splitting goes. As Gunnarsson has shown,¹⁰ minimization of the total energy requires that the chemical potentials ϵ_F^\uparrow and ϵ_F^\downarrow of the spin-up and spin-down electronic systems be equal. In terms of Fig. 1, this means that the spin-up and spin-down Fermi energies ϵ_F^\uparrow and ϵ_F^\downarrow must be separated by the product IM , where I is the Stoner exchange integral, an intra-atomic property. Equivalently, this means that the slope of the dashed chord in Fig. 1,

$$M/(\epsilon_F^\uparrow - \epsilon_F^\downarrow) \equiv \bar{n} = I^{-1}, \quad (1)$$

must equal the inverse of the Stoner parameter I . Since the slope of the dashed chord is simply the average state density¹⁰ in the energy region $\epsilon_F^\downarrow \leq \epsilon \leq \epsilon_F^\uparrow$, we see that the spin splitting starts if the Stoner condition $In(\epsilon_F^P) > 1$ is satisfied, and stops when $I\bar{n} = 1$, with \bar{n} defined by Eq. (1). Here $n(\epsilon_F^P)$ is just the slope of the integrated state density at ϵ_F^P . Figure 1 makes it clear that if I and the Fermi-level state density are large enough to make the magnetism strong, then the majority-spin Fermi energy will, in general, lie *above* the top of the d band.

We turn now to the question of the position of the ferromagnetic Fermi energy relative to a valley in the paramagnetic state density. In Fig. 2 we show a schematic state density exhibiting a parabolic minimum. In the lower half of the figure, we show the corresponding (cubic) integrated state density. As mentioned above in connection with Fig. 1, the total energy is minimized when \bar{n} , the slope of the dashed chord, equals the inverse Stoner exchange integral I^{-1} . Figure 2 shows us that the equilibrium Fermi energy is likely to fall in the vicinity of the state-density minimum, simply because values of the magnetization that bring the Fermi energy to this region cause the slope of the chord, considered as a function of the magnetization, to vary rapidly, i.e., to take on a wide range of values for a small variation of the magnetization. The distinction we are trying to make here is between energetic stability associated intrinsically with the state-density minimum on the one hand, and simple statistical likelihood on the other hand.

Another point to be made in this context is that, although the discussion of Fig. 2 focused on the majority-spin Fermi energy, these considerations are completely symmetric with respect to minority and majority spin. An analogous situation can arise if the paramagnetic Fermi energy falls *above* the state-density minimum. In this case, it is the minority-spin Fermi energy that is likely to fall near the minimum in the state density. Body-

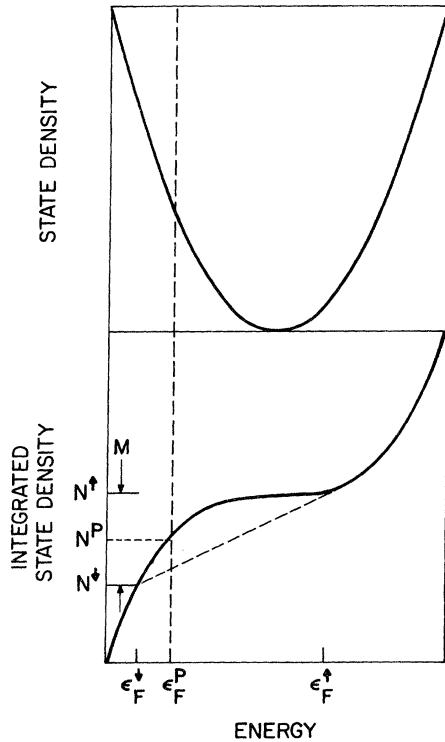


FIG. 2. Effect of a minimum in the paramagnetic state density on the position of the ferromagnetic Fermi level. Upper graph shows paramagnetic state density possessing a parabolic minimum. Lower graphs shows the corresponding (cubic) integrated state density. The total energy is minimized when the magnetization $M = \mu_{av} = N^\uparrow - N^\downarrow$ causes the slope of the chord in the lower graph $M/(\epsilon_F^\uparrow - \epsilon_F^\downarrow)$ to equal the inverse Stoner exchange integral I^{-1} , as in Fig. 1.

centered-cubic Fe is a well-known example of this situation because its d band is split into two main peaks separated by a deep valley.^{5,11} The exchange splitting shifts the minority-spin density of states so that the Fermi level falls in its gap. In this situation, both spin bands have holes.

It is appropriate at this point to define more specifically what we mean by strong magnetism. Strong magnetism refers to the condition where the Fermi level lies in a gap or low density-of-states region of *either* the spin-up or spin-down bands. The deeper the gap or the lower the density of states, the stronger the magnetism. This is because any perturbation to the system such as applied field or pressure will modify the magnetization very little. In effect, M is pinned on the plateau in the integrated density-of-states curve as shown in Figs. 1 and 2. Alternatively we can say that the Fermi level is pinned in the band gap. In this sense all the cases we have discussed, including the simple fully polarized spin-up band and also bcc Fe, are strongly magnetic. A narrower definition which we and others have used in the past is that the spin-up (majority) d band should be fully polarized. By such a definition, bcc Fe is weak.

III. HISTORICAL REVIEW

Let us consider an alloy $A_{1-x}B_x$ where A is the host (usually Fe, Co, or Ni) and B is the solute (either another transition metal or a metalloid). Quite generally, its atom-averaged moment in Bohr magnetons is the difference of the atom-averaged number of spin-up and spin-down electrons

$$\mu_{av} = \mu_A(1-x) + \mu_B x = N^\uparrow - N^\downarrow. \quad (2)$$

But the average electronic valence, that is, the number of electrons outside the last filled shell, equals the sum of spin-up and spin-down electrons

$$Z_{av} = Z_A(1-x) + Z_B x = N^\uparrow + N^\downarrow. \quad (3)$$

One can eliminate either N^\uparrow or N^\downarrow from these equations to obtain

$$\mu_{av} = 2(N_{sp}^\uparrow + N_d^\downarrow) - Z_{av} \quad (4)$$

or

$$\mu_{av} = Z_{av} - 2(N_{sp}^\downarrow + N_d^\uparrow), \quad (5)$$

where we have broken N into its sp - and d -band components.

Now let us consider some special cases. Assuming N_{sp}^\uparrow and N_d^\downarrow are constant under alloying (we shall return to discuss this assumption at length), and identifying the pure host moment as

$$\mu_A^0 = 2(N_{sp}^\uparrow + N_d^\downarrow) - Z_A, \quad (6)$$

we find from Eq. (4)

$$\mu_{av} = \mu_A^0 - x(Z_B - Z_A). \quad (7)$$

On the other hand, assuming both N_{sp}^\downarrow and N_d^\uparrow are constant and redefining μ_A^0 in a way analogous to Eq. (6), we find

$$\mu_{av} = \mu_A^0 + x(Z_B - Z_A). \quad (8)$$

Comparison with Eq. (7) shows a change of sign in the concentration dependence. This sign change is the origin of the well-known triangular shape of the traditional Slater-Pauling curve, whose right side has a downward 45° slope and whose left side has an upward 45° slope versus average valence. In other words, the two sides correspond to either spin-up or spin-down electron numbers remaining constant.

With this background we are in a position to review some early theories of strong ferromagnetism, so as to set the band-gap theory in proper perspective. The earliest and most widely used theory of strong ferromagnetism was the rigid-band theory.^{2,12,13} It presumes that the d bands as well as the sp bands of the alloy form common bands, invariant under alloying. These common bands are filled by electrons according to the average chemical valence. For conventional strong ferromagnets the theory assumes that spin-up d band is full; so N_d^\uparrow does not change with alloying and $2N_d^\uparrow = 10$ in Eq. (6). In his original work, Mott² also took N_{sp}^\uparrow as constant, although he had more difficulty justifying this assumption. Thus he obtained Eq. (7), which became known as a rigid-band formula, even though this is not the only way to derive the

result as we shall see below. This simple equation works well for Ni-Cu, Ni-Zn, Ni-Co, Co-rich Fe-Co, and Ni-rich Fe-Ni. These alloys form the right-hand side downward sloping portion of the conventional Slater-Pauling curve.¹²⁻¹⁵

An equally simple theory has been applied to bcc Fe-based alloys.^{5,11} Alloys such as Fe-Cr and Fe-rich bcc Fe-Co are assumed to form rigid bands with a gap in the bcc spin-down band. For clarity, we emphasize that Cr and Co were assumed to have the same density of states with the same gap as Fe; we are not talking about a gap between a Cr subband and an Fe subband. If the Fermi level is pinned in the gap of the spin-down band of these alloys, just as for Fe, N_d^\downarrow will remain constant under alloying. If N_{sp}^\downarrow also remains constant, one has the result of Eq. (8). This theory explains the bcc Fe-rich Fe-Co and Fe-Cr alloys, and perhaps Fe-V also. These alloys form the left-hand-side upward-sloping portion of the Slater-Pauling curve.

In spite of these remarkable successes, rigid-band theory soon ran into trouble. As theorists improved their calculational techniques, and experimentalists developed more sophisticated probes of band structure, such as photoemission, it became clear that the bands were simply not rigid, even for the simplest cases.^{16,17} This led researchers to label the rigid-band theory "completely wrong" and its "success based on canceling mistakes."¹⁷ Although we agree that the bands are not rigid, we believe that Eqs. (7) and (8) are essentially correct for many systems. The reason can be seen from Eqs. (4) and (5): The magnetic moment depends only on *total* numbers of *sp* and *d* electrons, not on the band shape. Although rigid-band theory implies the constancy of these numbers under alloying, *the reverse is not necessarily true*. As we shall see shortly, there is, in fact, a much deeper reason for this constancy, which goes beyond rigid-band theory and arises simply from the existence of the gap. Unfortunately, the misconception that rigid-band theory is necessary (as well as sufficient) to obtain these results has clouded many discussions of alloy magnetism.

The first major modification of the rigid-band picture came from the work of Friedel,⁶ who recognized that in mixtures of early and late transition metals, the relatively repulsive *d* potential on the early transition-metal solute created a separate high-energy *d* band containing precisely ten states per solute. When, as frequently occurs, the spin-up Fermi level is pinned in the gap between the solute and host subbands, then Eqs. (4) and (7) are modified to

$$\mu_{av} = \mu_A^0 - x(10 + Z_B - Z_A), \quad (9)$$

provided also that N_{sp}^\uparrow continues to remain constant. This theory accounted for many of the non-45°-slope subbranches on the Slater-Pauling plot, such as Co-Cr, Co-V, Ni-Cr, and Ni-V.

While these theories provide a succinct account of the magnetization of all the strongly magnetic alloys composed exclusively of transition metals, it is not at all clear how to generalize the analysis to alloys containing metalloids. Although each metalloid replacing a transition metal must reduce the number of occupied spin-up *d* states by

5, the new issue introduced by metalloids is the questionable constancy of N_{sp}^\uparrow , the number of spin-up *sp* electrons. Whereas the valence-band structure of all transition metals is fundamentally similar, making the notion of a constant N_{sp}^\uparrow plausible, the valence bands of alloys containing metalloids are fundamentally different: The valence bands of these materials reflect the fact that elements on the right-hand side of the Periodic Table are characterized by completely filled *s* shells and substantially filled *p* shells. It may therefore seem astonishing if Eq. (9), which is based on the constancy of N_{sp}^\uparrow , were to apply without modification to alloys containing B, Al, and Si, for example. Yet the experimental results for Ni-Al, Ni-Ge, Ni-Si, and Ni-Sb are famous in this regard. In fact, Mott² recognized from the very beginning that these data imply the constancy of N_{sp}^\uparrow . The coincidental fact that the valence *Z* of Ni is 10 gives Eq. (9) a particularly simple form *when it is specialized to Ni*:

$$\mu_{av} = \mu^0 - xZ_B. \quad (10)$$

Textbooks^{14,15} have continued to refer to the simple valence dependence of the nickel-alloy data without clearly specifying either the underlying assumptions or the formula. This has led to confusion with regard to the interpretation of Co-alloy data, for which Eq. (9) does not reduce to Eq. (10), because of the valence difference between Co and Ni. Yet all too often Eq. (10) has been mistakenly applied to the Co alloys. Another notion, particularly common in the literature on amorphous ferromagnets, is that metalloid solutes can contribute their valence electrons to the minority-spin bands of the transition-metal host. This variant of rigid-band theory (the host bands are rigid and metalloid bands are ignored) is commonly called the "charge-transfer" model.¹⁸⁻²³ By rejecting the older notion of constant N_{sp}^\uparrow , and assuming that all the *sp* electrons are transferred to the transition-metal atoms, one is led to the following (in our view incorrect) formula for the magnetization:

$$\mu_{av} = \mu_A^0 - x(\mu_A^0 + Z_B), \quad (11)$$

where Z_B is the metalloid valence. The different physical assumptions underlying Eqs. (9) and (11) are reflected in a difference of $2N_{sp}$ in the coefficient of *x*, that is, in the slope of the concentration dependence of the magnetization. The form of Eq. (11), more specifically the factor of $1-x$ multiplying the host magnetization, led to yet another unfortunate turn in the history of this subject, namely, the shift in focus from the average magnetization per alloy atom to the magnetization per transition-metal atom:

$$\mu_A = \mu_A^0 - Z_B x / (1-x). \quad (12)$$

This formula has the attraction of predicting that the slope of the concentration dependence of the magnetization should be an integer, at least at low concentrations. In practice, the coefficient of *x* in Eq. (12) has been treated as an adjustable parameter, and measured data have been interpreted as indicating the number of electrons supplied by each metalloid to the transition-metal bands. Of course, by treating Z_B as a fitting parameter, the predic-

tive power of Eq. (11), aside from its linearity, is lost.

Doubts about rigid-band theory in any form have spawned yet another school of thought focusing on the detailed bonding in metal-metalloid clusters.^{17,24,25} The covalent bonding causes hybridization of host d states with metalloid sp states and in effect makes them magnetically inactive. Attempts have been made to estimate the hybridization effect and relate it to experiment on both amorphous and crystalline alloys.²⁵ Noteworthy predictions of this approach are a sensitive dependence of moment on local environment and, to the extent that the solute environment is similar, an independence of solute valence for Co alloys.

A related approach²⁶ seeks to explain variations in the Fe moment on the basis of chemical short-range order. If the heat of mixing or heat of compound formation is large, leading to clustering of unlike atoms, the iron tends to have more metalloid neighbors, and its moment is assumed to drop. NMR and Mössbauer studies have shown evidence for such local-environment effects.¹⁷

There is nothing wrong with the hybridization and local-environment models provided they are treated with sufficient precision to obtain usefully accurate results. The problem is that they obscure an underlying simplicity of the experimental data which the original rigid-band theory had identified. They also imply a sensitivity of the *net* moment to the local geometric and chemical environment, while in our view, the net moment (in contrast to the local moment) is not very sensitive as long as strong magnetism prevails.

IV. BAND-GAP THEORY

The fundamental mystery concerning the effect of metalloids on transition-metal magnetism was eliminated in 1971, when Terakura and Kanamori^{3,4} showed for the case of Ni alloys how it is possible that metalloid solutes can leave the number of sp electrons unchanged, and therefore why the magnetization of metalloid alloys can be described by Eq. (9). The work of Terakura and Kanamori is particularly convincing in that, not only is a physical mechanism proposed that accounts for the experimental data, but the effectiveness of the mechanism in holding the number of sp electrons constant is demonstrated by direct calculation. As a preliminary, we point out that our self-consistent energy-band calculations are completely unequivocal with regard to both the near neutrality of the metalloid atoms, even when they are dissolved in a transition-metal lattice and the intuitive reasonableness of the electronic structure of each metalloid atom (in particular, their s shells are filled).²⁷ The paradox resolved by the work of Terakura and Kanamori is how the metalloids can have a larger number of sp electrons than typical transition metals without increasing the value of N_{sp}^{\uparrow} appearing in the expression for the magnetization [Eqs. (6) and (9)].

The resolution of the paradox rests on two independent points. First, two mechanisms exist by which the valence s and p states of the metalloid can be created. One is that new sp states (that is, states in addition to those originally below the Fermi level) are simply pulled down below the

Fermi level by the attractive potential of the metalloid and filled with electrons. We call this the "new-state filling" mechanism, which leads to a change in N_{sp}^{\uparrow} . But there is an alternative to this simple filling of states that are unoccupied in the host. The alternative mechanism is the "polarization" of neighboring occupied states of the host. That is, states centered on the solute are made up from linear combinations of states originally centered on nearest-neighbor sites. In this case there is no change in N_{sp}^{\uparrow} , because the metalloid states are made up of states which are already below the Fermi level and therefore already filled.

The second crucial observation of Terakura and Kanamori is the reason that polarization tends to occur more than new-state filling in these systems. The response of any system to a perturbing field, such as the relatively attractive s -electron potential of the metalloids, depends primarily on the availability of states possessing the correct symmetry and spatial distribution to "feel" the perturbation. If there is a gap in the spectrum of such states, then the potential must be very strong to displace states across the gap. The important property of the host electronic structure in this context is that hybridization of the sp states with the d states results in a depression near the Fermi level of the density of sp states, that is, states that might respond to the stronger metalloid sp potential. It is this approximate gap in the sp state density that acts to hold N_{sp}^{\uparrow} nearly constant, by forcing the transition-metal host to screen the metalloid sp potential by means of the polarization mechanism. This "hybridization gap" is well known in the context of transition-metal electronic structure; it is referred to by Terakura and Kanamori as a "Fano-antiresonance" effect and, by any name, it is exhibited²⁸ for Co in Fig. 3.

We emphasize that the sp gap due to hybridization is not perfect, and that metalloids, especially those with high valence, can cause N_{sp}^{\uparrow} to increase somewhat, as will be discussed further in Sec. V. We shall also see that N_{sp}^{\uparrow} appears to have an observable structure dependence. The fact that these effects are occasionally as large as the magnetization variations of experimental interest should not, in our view, obscure the tremendous simplification that the implications of the near constancy of N_{sp}^{\uparrow} bring to the entire field of transition-metal magnetism.

Of course, the presence of a gap has the added feature that either the spin-up or the spin-down Fermi level of a ferromagnet tends to fall in the gap, as we have shown in Sec. II. Then the states below the gap will all be filled with electrons. Thus *state* conservation translates to *electron-number* conservation. This explains the success of the old rigid-band theory and is the underlying principle of our more general band-gap theory.

To compare the band-gap theory to experimental data on metal-metalloid systems, it is conventional to plot average moment versus solute concentration, with different slopes corresponding to different solute valences and shifting zero-concentration intercepts corresponding to small shifts in spin-up sp electrons. To reveal these effects in a more consistent manner, and at the same time to permit simultaneous treatment of ternary fcc and amorphous alloys, we have proposed⁸ a generalized Slater-Pauling plot

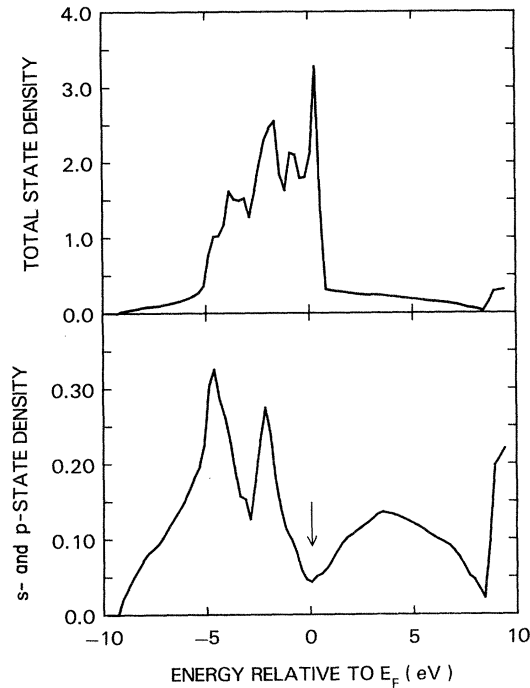


FIG. 3. Paramagnetic (non-spin-polarized) sp and d densities of states of fcc cobalt, from self-consistent band calculations, after Moruzzi *et al.* (Ref. 28). Note the difference in scales for the sp and d densities. The arrow indicates the hybridization gap which helps hold $2N_{sp}^{\uparrow}$ constant as described in the text.

of average alloy moment (per all atoms) versus average magnetic valence

$$Z_{m,av} = \sum_i x_i Z_m^i, \quad (13)$$

where x_i is the atom fraction and $Z_m^i = 2N_{di}^{\uparrow} - Z^i$ is the magnetic valence (Z^i being the electronic valence) of the i th constituent. If i is a metalloid, $2N_{di}^{\uparrow} = 0$. As mentioned above, dilute bcc Fe alloys require different treatment, but if the spin-up d band becomes full (in concentrated alloys, as we shall see below), Eq. (13) again applies.

In the generalized Slater-Pauling plots⁸ to be shown in Figs. 6–19, a series of data lying parallel to the line $\mu_{av} = Z_m + 0.6$ indicates strong magnetism. A parallel shift from this line suggests a shift in the number of spin-up sp electrons from $0.3 = 0.6 \div 2$, the number for Fe, Co, and Ni. Such shifts, up to $0.45 = 0.9 \div 2$, appear to occur for amorphous alloys of Fe and Co with early transition metals,⁷ and, as we shall see in the next section, comparable shifts are expected for fcc-like metalloid systems. A series of data lying below the line, and especially with different slope, indicates weak magnetism, that is, incomplete filling of the spin-up d band up to the gap; in this case two times the number of spin-up d electrons is reduced from 10 in Eqs. (6) and (9). A series of data which fall below the line for very small solute concentrations, as in the case of bcc Fe alloys, but shift closer to the line with solute addition and eventually curve over parallel to it at higher concentrations, indicates the development of

strong magnetism with a filled spin-up band. We shall discuss many examples of these behaviors in Sec. VI.

Another important point is that the band-gap theory for the net moment of strong ferromagnets is relatively structure insensitive because concentration dependences are entirely controlled by chemical valences in Eq. (9). (The only structure sensitivity in the net moment comes, as we shall see below, from N_{sp}^{\uparrow}). We know, of course, that the local environments of alloys are quite complex and that different sites can have different moments, depending, for example, on the number of metalloids surrounding a given transition metal. For example, in the case of an earlier calculation²⁹ on bcc Fe_3Si , the two different Fe sites were found to have different moments. But the local band structures of both sites showed fully polarized spin-up d bands, and in this case the band-gap formula will still apply for the *net* magnetization. Another example is provided by calculations⁷ on fcc Fe_3Zr and Fe_3Ti , in which the early transition metal shows an antiferromagnetic moment, and yet once again, the net result is just Eq. (9).

Thus the band-gap theory is not inconsistent with experimental observations of local-environment effects, but rather it offers a sort of conservation or sum rule which governs the net result. However, this implies a warning about simplified models based on the local environment or hybridization pictures. Usually such models imply that different local structure can lead to different net moments. We believe such a prediction is often wrong. For as long as the system is a strong ferromagnet, we shall see that experiment amply supports the structure insensitivity predicted by the band-gap theory.

V. EXTENSION TO HIGH CONCENTRATION

At high concentration (~ 25 at %) of metalloid, where metalloids are no longer isolated impurities, one might expect such state-density features as the sp -band gap in Fig. 3 to fill in or become more diffuse because of the variety of local environments in disordered alloys. In what follows, however, we argue that such a gap could actually become deeper and better defined. If this is true, it would significantly expand the range of alloys described by the theory to include both concentrated crystalline Fe alloys with metalloids and also the important group of Fe- and Co-metalloid glasses which typically occur in the 20–25 at. % concentration range. While many other explanations have been proposed for the magnetism of these systems, none of them, to our knowledge, has hit on the simple band-gap theory, which we believe explains the results better and on a more physical basis. The theory also explains structure insensitivity, that is, why amorphous and crystalline materials of the same composition usually have such similar moments. And finally, it explains why such a preponderance of magnetic systems are strong.

Evidence for the gap at higher concentrations comes from our crystalline band-structure calculations, which, as described elsewhere, are self-consistent and use the local-spin-density approximation of exchange and correlation as well as the efficient augmented spherical-wave method.³⁰ We have performed such calculations on a variety of A_3B systems in the fcc Cu_3Au and bcc Fe_3Si structure where

$T=Fe, Co,$ and Ni and $M=B, C, N, Al, Si, P, Ga, Ge,$ and Sn as well as various early transition metals. We have already reported⁷ on the calculations with early transition metals, where it was found that a lower total state density appears immediately above the Fe d bands in the 3:1 compositions, say of Fe_3Zr , than in Fe itself. We have also reported on spin-polarized calculations of bcc Fe_3Si , which is a strong ferromagnet with a state-density dip (gap) at the spin-up Fermi energy.²⁹ In Fig. 4 we show the results of paramagnetic (not spin-polarized) calculations of fcc Co_3Si . Here too a well-defined dip or gap, indicated by the arrow, occurs in the sp state density. This is typical for all the metalloids mentioned above. The results of a spin-polarized calculation on Fe_3B are shown in Fig. 5. The state densities are very similar to those of the corresponding paramagnetic calculation, with spin-up and spin-down bands shifted roughly rigidly down and up, respectively, relative to the Fermi energy. Just as discussed in Sec. II, the Fermi level falls in the gap of the spin-up band.

Comparison of Figs. 3 and 4 shows that, much as in the case of Fe and Fe_3Zr discussed in Ref. 7, there is a characteristic and significant change of the d -band state density in Co_3Si from that in Co. Instead of a sharp peak at the top of the d band in Co, the d band of Co_3Si rises more gradually below the gap, and the gap becomes *better* defined than in Co. This suggests that in the alloy there is a gradual change from one type of band structure to the other type as a function of solute. This change is likely to occur around 10% in close-packed alloys, because by this concentration, every transition-metal atom has a solute neighbor on the average.

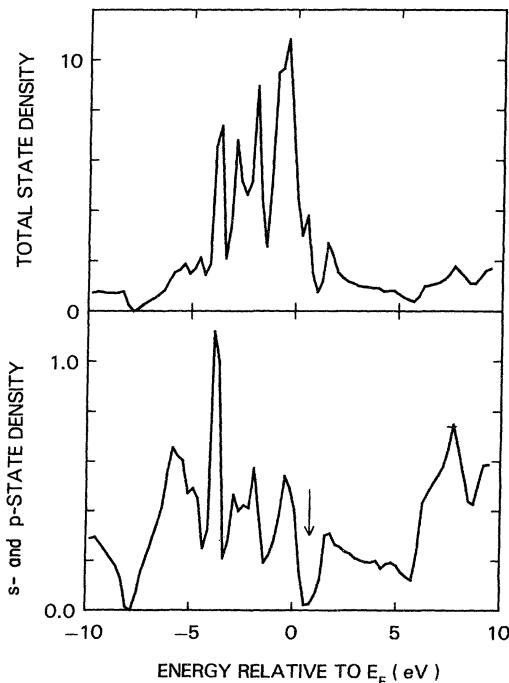


FIG. 4. Paramagnetic (non-spin-polarized) sp and d densities of states on the cobalt site of Co_3Si in the Cu_3Au fcc structure. Note the difference in scales for the sp and d densities. The arrow indicates the gap discussed in the text.

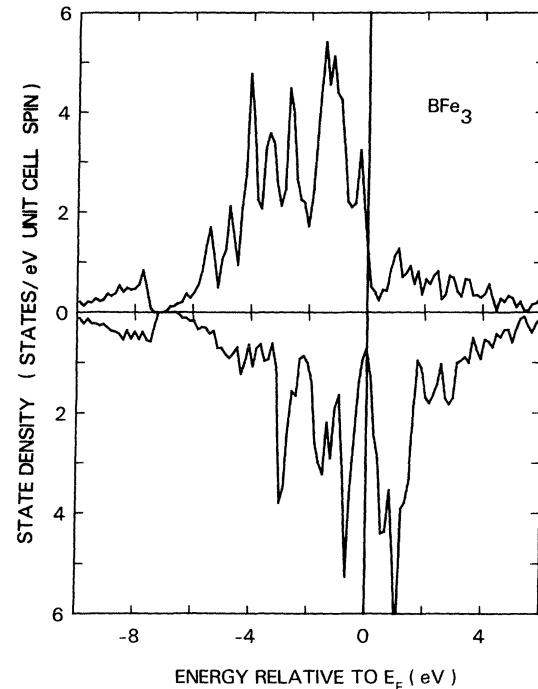


FIG. 5. Total state density for spin-up and spin-down electrons in Fe_3B in the Cu_3Au (fcc-like) structure. The system exhibits strong magnetism in that the Fermi level falls in the gap above the majority-spin d states. The state density is quite typical of those given by our calculations for alloys containing Fe, Co, and Ni with metalloids. The degree of d -band polarization for these 3:1 alloys varies with volume, and is often incomplete for the volume that minimizes the total energy.

An integration of the paramagnetic state density up to the "gap" in Fig. 4 gives a net of 34 ± 0.2 states per formula unit or 8.5 per atom, for a surprisingly large number of fcc systems, as listed in Table I (except for pentavalent solutes where the gap is less well defined). Since the three transition-metal atoms per formula unit contribute 30 d states, this leaves 4 sp states per formula unit or 1 sp state

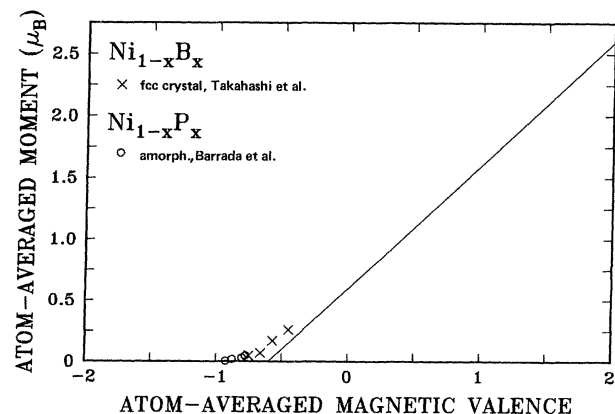


FIG. 6. Generalized Slater-Pauling plot of atom-averaged moment vs atom-averaged magnetic valence [see Eq. (13) in text] for the Ni-B and Ni-P alloy systems. Data from Refs. 32 and 33.

TABLE I. Paramagnetic band calculations in the Cu_3Au structure.

System (A_3B)	Lattice parameter (a.u.)	Integrated state density to gap (per formula unit)
Fe_3B	6.27	34.3
Fe_3Si	6.54	34.2
Fe_3P	6.49	32.0
Fe_3Sc	6.83	33.9
Fe_3Ti	6.72	33.9
Fe_3Y	7.10	33.9
Fe_3Zr	6.97	33.9
Fe_3Nb	6.87	33.9
Co_3Al	6.61	34.1
Co_3B	6.26	34.1
Co_3Si	6.54	34.2
Co_3P	6.48	32.3
Co_3Sc	6.81	33.9
Co_3Ti	6.69	33.9
Co_3V	6.61	33.8
Co_3Y	7.07	33.9
Co_3Zr	6.93	33.9
Co_3Nb	6.84	33.9
Ni_3Al	6.68	34.1
Ni_3Si	6.61	34.2
Ni_3V	6.71	33.9
Ni_3Cr	6.64	33.8
Ni_3Nb	6.93	33.9
Ni_3Mo	6.86	33.8

per atom. Since roughly half of these are spin up, we predict $2N_{sp}^\uparrow = 1$ per atom for these systems. Fcc spin-polarized calculations support this number, as shown in Table II, where certain compounds have been calculated with an expanded, nonequilibrium lattice to ensure strong magnetism. Crystalline bcc compounds and alloys have a characteristically different state density with the two-peak structure characteristic of bcc Fe ,^{29,31} but a similar tendency for an sp gap at the top of the d bands. The calculations on bcc Fe_3Si imply a value $2N_{sp}^\uparrow$ of 0.8 (see Table I), which is lower than the typical fcc value of 1.

Admittedly, all these results are for crystalline compounds, not disordered alloys. But we note that gaps occur both for bcc and fcc structures and at 0 and 25 at. % (though not at 50 at. %) metalloid. This suggests that gaps are a rather general feature of the low to middle

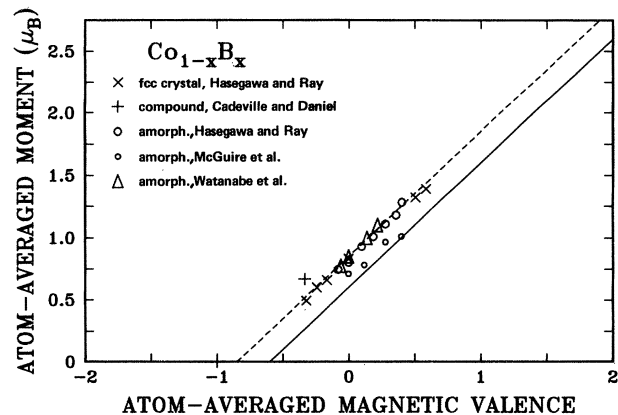


FIG. 7. Generalized Slater-Pauling plot for Co-B alloys with data from Refs. 37–39, and 58.

composition range, and relatively independent of the kind of local structures typically present in metallic glasses or crystalline alloys. In the absence of more explicit band calculations on such disordered structures, we will proceed with this assumption and use experiment as the final arbiter of its validity.

From these results we can begin to piece together the pattern which a full alloy system might be predicted to follow. We associate the different values of $2N_{sp}^\uparrow$ with the different types of band structures: 0.6 for the pure host and the very dilute ($< 10\%$) fcc alloys, 1 for fcc alloys in the range of 25% solute, and 0.8 for bcc alloys in the same range. Since transition metals in amorphous alloys typically have ~ 12 nearest neighbors, we consider them to be fcc-like, and therefore we expect amorphous alloys in the 25% range to show $2N_{sp}^\uparrow \sim 1$ also.

Now let us consider the change of $2N_{sp}^\uparrow$ from 0.6 to 1 in fcc alloys as solute concentration increases from 0 to 25 at. %. The transition metal which each metalloid replaces had 0.6 sp electrons; so at the 3:1 composition $4(1-0.6) = 1.6$ new sp states have been introduced below the gap per formula unit. This is what we have called new-state filling. But for charge neutrality, a trivalent metalloid requires three sp electrons, which means that $3 - (1.6 + 0.6) = 0.8$ sp states on the metalloid have been created by what we have called the polarization mechanism. For a tetravalent metalloid, 1.8 sp states will be created by polarization. The comparison of 1.6 new sp states and 0.8 or 1.8 polarization states gives some measure of the relative effectiveness of the polarization and

TABLE II. Spin-polarized band calculations (eq. means equilibrium; exp. means expanded).

System (A_3B)	Structure	Lattice parameter (a.u.)	μ_{A1} (μ_B)	μ_{A2} (μ_B)	μ_B (μ_B)	μ_{av} (μ_B)	$2N_{sp}$
Fe_3B	fcc	6.58 (exp.)	2.32		-0.23	1.68	0.93
Fe_3Si	fcc	7.032 (exp.)	2.18		-0.17	1.59	1.09
Fe_3Si	bcc	10.69 ^a (eq.)	2.48	1.36	-0.09	1.28	0.78
Co_3Si	fcc	6.937 (exp.)	1.08		-0.18	0.765	1.015
Co_3Sn	fcc	7.266 (exp.)	1.10		-0.10	0.8	1.05

^aThis lattice parameter corresponds to 16 atoms per unit cell.

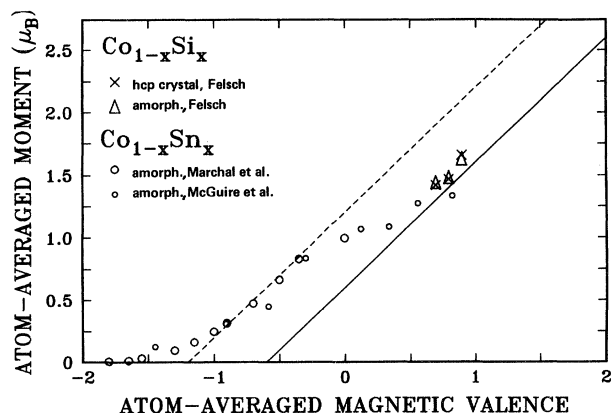


FIG. 8. Generalized Slater-Pauling plot for Co-Si and Co-Sn alloys with data from Refs. 40, 42, and 43.

new-state-filling mechanisms. Clearly filling cannot be ignored and it will cause significant deviations in the alloy moment away from the Slater-Pauling 45° line.

At this point the question reduces to how these numbers change as a function of composition. If these effects depend nonlinearly on concentration and alternate from one to the other, new-state filling may be dominant in certain regions of concentration while polarization may be dominant in others. In particular, because of the well-defined gap we observe in the 3:1 compound, we anticipate that in a range around this alloy composition the polarization mechanism will dominate and the moment data will parallel the Slater-Pauling 45° line. As we shall see, this supposition is borne out by experimental data on many systems. There is also reason to believe, on the basis of the Ni-alloy calculations of Terakura and Kanamori^{3,4} as well as experimental data, that the polarization mechanism dominates in dilute (< 10%) Ni alloys, although it is not yet clear to what extent this applies to Co and Fe alloys. If indeed polarization dominates around 0 and 25 at. %, then filling must dominate between, most probably around 10 at. %, where the changeover in band structure occurs as described earlier.

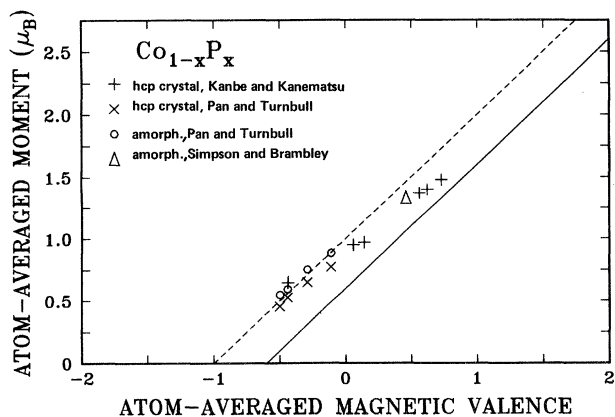


FIG. 9. Generalized Slater-Pauling plot for Co-P alloys with data from Refs. 34–36.

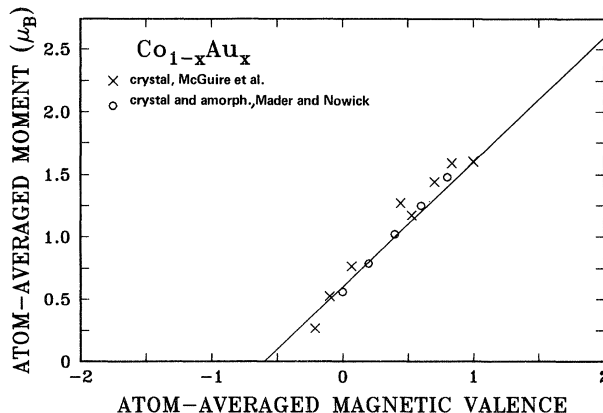


FIG. 10. Generalized Slater-Pauling plot for Co-Au alloys with data from Refs. 44 and 45.

In summary, the details of this picture remain to be substantiated by explicit calculation at different concentrations and by further experimental results, but a plausible expectation based on our present results is as follows: As we add metalloid to an fcc or fcc-like amorphous host, we may expect the alloy moment initially to shift down parallel to the line $\mu_{av} = Z_{m,av} + 0.6$ on a generalized Slater-Pauling plot. But as the concentration approaches 10 at. %, we expect the data to shift upward toward the line $\mu_{av} = Z_{m,av} + 1$, and, in the range of 25 at. % solute concentration, to curve over and run parallel to it. The mechanism will fail near 50 at. % solute concentration because we observe no gap in our calculations at the 1:1 composition. But by this point most alloys are predicted to be nonmagnetic anyway, because both spin-up and spin-down d bands will be full. By contrast the crystalline bcc alloys should parallel a somewhat lower line corresponding to $2N_{sp}^{\uparrow} \sim 0.8$. Aside from the weak difference in N_{sp}^{\uparrow} between fcc and bcc alloys, the concentration dependence in the band-gap theory formulas of Eqs. (6) and (9) is structure independent.

This discussion has neglected two other complications. One is the appearance of holes in the Fe spin-up band as

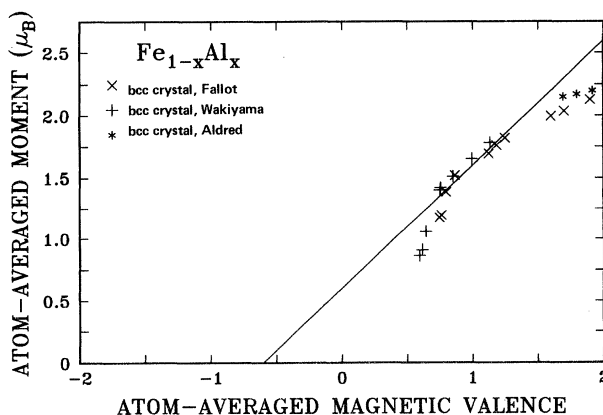


FIG. 11. Generalized Slater-Pauling plot for Fe-Al alloys with data from Refs. 46, 47, and 49.

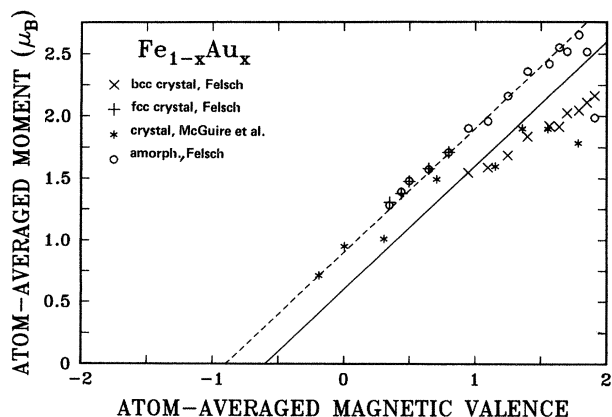


FIG. 12. Generalized Slater-Pauling plot for Fe-Au alloys with data from Refs. 44 and 51.

one lowers the metalloid concentration toward pure Fe. This effect is surprising because one might expect the strength of the magnetism to increase as one removes the nonmagnetic metalloid and approaches pure Fe. This has already been discussed elsewhere.⁷ A second complication is the appearance of antiferromagnetism or spin-glass behavior, as in Ni-Mn or in Fe-Al at high Al concentration. Both these effects cause the moment data to curve downward, away from the Slater-Pauling line. Both can be structure sensitive. Both deserve much detailed discussion, which we reserve for later work, but they must be borne in mind as we review the experimental data.

VI. COMPARISON TO EXPERIMENT

The most spectacular support for the band-gap theory comes from the crystalline fcc Ni-metalloid alloys.^{1,2,14,18} We have recently reviewed these data using the generalized Slater-Pauling construction,⁸ and do not repeat them here. The data show no significant tendency to shift away from $2N_{sp}^{\uparrow} \sim 0.6$. This is consistent with our hypothesis in the preceding section that $2N_{sp}^{\uparrow} \sim 0.6$ should apply in the dilute limit. Indeed, the Ni-Al, Ni-Si, and other metalloid

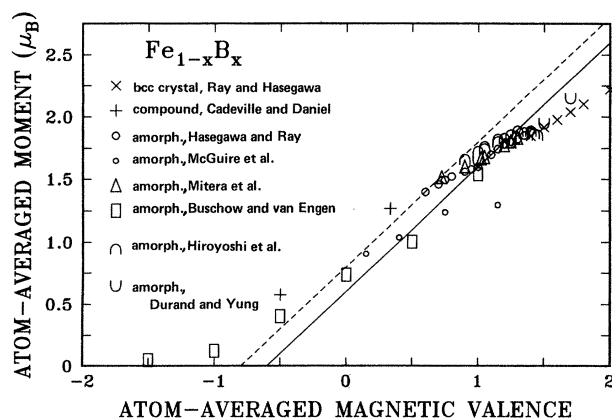


FIG. 13. Generalized Slater-Pauling plot for Fe-B alloys with data from Refs. 18 and 52–59.

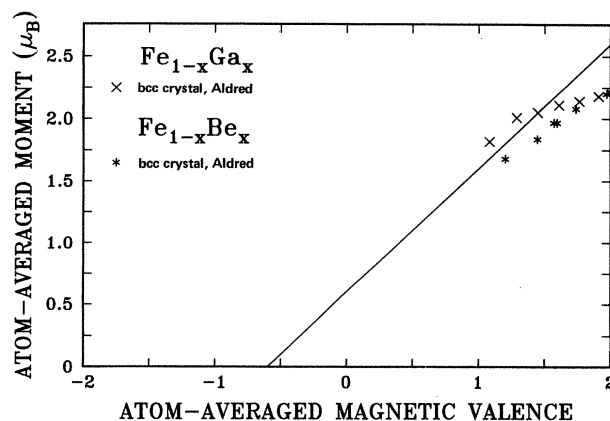


FIG. 14. Generalized Slater-Pauling plot for Fe-Ga and Fe-Be alloys with data from Ref. 47.

alloys are quite dilute. Ni-Zn and Ni-Cu are more concentrated, but these do not show a metalloid-like band structure. New data on concentrated amorphous Ni alloys^{32,33} with B and P are shown in Fig. 6. They indicate $2N_{sp}^{\uparrow} \sim 0.7$, and a slope in agreement with Eq. (10), but the result is complicated by a tail at high concentrations (low Z_m) which is presumably due to Ni clusters in the critical range where the average moment is approaching zero.

Turning to the Co alloys, we emphasize that the data are to be compared with Eq. (9) [not Eq. (10) as has occasionally been done in the past^{15,34–36}]. Terakura and Kanamori³ were the first (and only ones to our knowledge) to do this, and the amount of data has expanded significantly since their work. Results^{34–43} on Co-B, Co-Si, Co-Sn, and Co-P are shown in Figs. 7–9. The Co-B data, both amorphous and crystalline, agree beautifully with the theory, with $2N_{sp}^{\uparrow} \sim 0.8$. The Co-Si data are at low Si concentrations where N_{sp}^{\uparrow} is expected to be close to 0.6, as observed, and amorphous and crystalline data are the same. Co-Sn appears to show the transition to the higher N_{sp}^{\uparrow} value, in this case close to 1.1, with a small region of the correct slope before a low moment tail develops at higher concentrations. Similarly, Co-P approaches the theoretical slope with $2N_{sp}^{\uparrow} \sim 1.0$ at moderate P concentration.

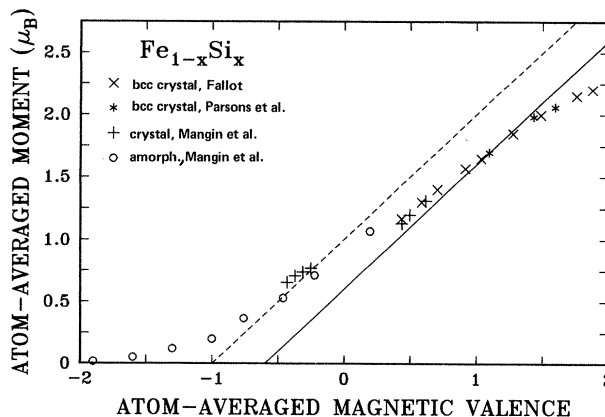


FIG. 15. Generalized Slater-Pauling plot for Fe-Si alloys with data from Refs. 41, 46, and 60.

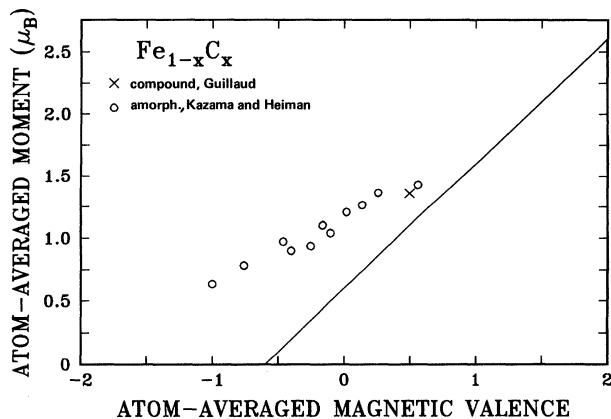


FIG. 16. Generalized Slater-Pauling plot for Fe-C alloys with data from Refs. 61 and 62.

For completeness we also include data^{44,45} on Co-Au, which also shows structure insensitivity and the correct slope but a somewhat lower $2N_{sp}^1 \sim 0.6$ (see Fig. 10), which contrasts with the Fe-Au result to be described below. The difference may be due to the strong tendency of Co-Au to phase separate, but this has not been directly confirmed in the existing studies.

Turning to the iron alloys, we find a remarkable historical blindspot. Little effort has been made to compare the data to any theory involving a valence dependence. The reason is easy to see with the example of the bcc Fe-Al data^{41,46-48} shown in Fig. 11. Up to 20 at. % Al, the data follows a so-called "dilution model"; this is the region of incomplete polarization of the spin-up d band, that is, of weak magnetism. Above about 25 at. % an abrupt decrease in the spontaneous magnetization and increase in the high-field susceptibility indicate either spin-glass behavior or the onset of weak magnetic behavior.^{31,48,49} These phenomena have diverted attention from the intermediate region between 20 and 25 at. % (Z_m from 1 to 0.75), where, in our opinion, strong ferromagnetism prevails. The only efforts to explain this behavior have been on the basis of a localized model with antiferromagnetic

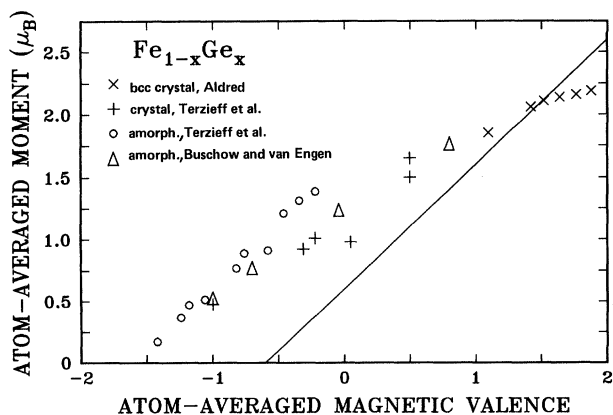


FIG. 17. Generalized Slater-Pauling plot for Fe-Ge alloys with data from Refs. 47, 55, and 63.

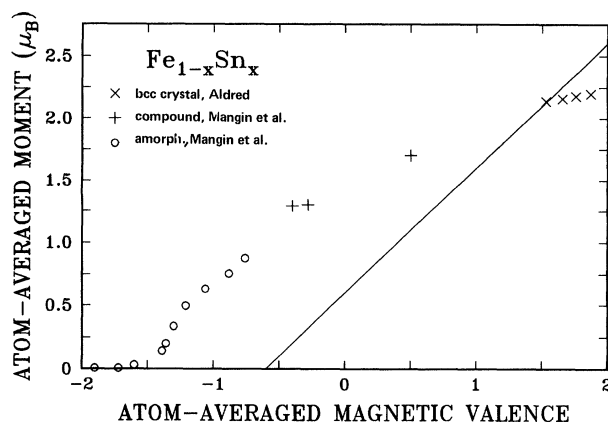


FIG. 18. Generalized Slater-Pauling plot for Fe-Sn alloys with data from Refs. 47 and 65.

interactions,⁴⁸ or on the basis of a local-environment effect.⁵⁰ This is the region we can explain so simply on the basis of the band-gap formula as shown in Fig. 11. The value of $2N_{sp}^1$ is close to 0.6, not far from our calculated value of 0.8 for bcc alloys. Although there is a dependence of the moment on local order even in this region,⁴⁸ the effect is weak in the context of our model, and arises from local clusters with higher Al concentration and consequent spin-glass behavior.

The tendency of the average moment to curve upward toward the band-gap theory line with solute addition seems universal in all the Fe-alloy data which we now review. The most spectacular example^{44,51} is the Fe-Au data shown in Fig. 12. Crystalline fcc and amorphous data lie on top of each other and agree beautifully with the theory, indicating $2N_{sp}^1 = 0.9$, over a wide concentration range. Most remarkable is the abrupt increase to strongly magnetic behavior with very small additions of Au in the amorphous matrix, which compares to a very gradual rise in the bcc crystalline Au alloys. Clearly this effect—the disappearance of weak magnetism with alloy addition—is strongly structure dependent.

Data^{18,52-59} on Fe-B is shown in Fig. 13. The different

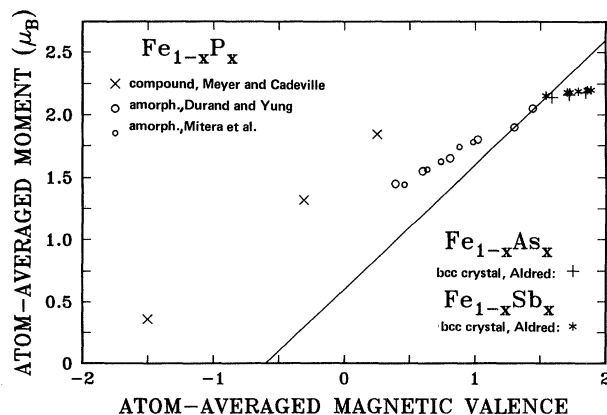


FIG. 19. Generalized Slater-Pauling plot for Fe-P, Fe-As, and Fe-Sb alloys with data from Refs. 47, 53, 58, and 66.

TABLE III. Values of $2N_{sp}^{\uparrow}$ from comparison of experimental average moment data in the 25% composition range to the band-gap theory of Eqs. (6) and (9). Dots indicate no data are available in the 25% concentration range. A *d* indicates disagreement with band-gap theory (wrong slope).

Solute	Fe				Co	
	bcc	fcc	Amorphous	hcp	Amorphous	
Au	...	0.9	0.9	0.6	0.6	
B	0.7	0.8	0.8	
Al	0.6	
Ga	0.7	
Si	0.7	1	1	
Sn	1.6(?)	...	1.1	
P	<i>d</i>	0.9	1.0	

data sets show downward deviations setting in at different concentrations, suggesting again the sensitivity of magnetic weakness to some structural feature of the different materials. But all the data converge on a line which agrees well with the theory, using $2N_{sp}^{\uparrow}=0.8$, over a wide concentration range. Data⁴⁷ on bcc Fe-Ga (Fig. 14) also roll over parallel to the theory with $2N_{sp}^{\uparrow}\sim 0.7$.

Turning to the tetravalent solutes, we find that Fe-Si in Fig. 15 has a behavior^{41,46,60} reminiscent of Fe-Au in that fcc and amorphous data are shifted higher ($2N_{sp}^{\uparrow}\sim 1$) than bcc data ($2N_{sp}^{\uparrow}\sim 0.7$). The concentrated bcc Fe-Si slope is well predicted by the theory but the amorphous data curve above the line, presumably because of clustering effects as mentioned above in the cases of Ni-B and Co-Sn.

The other tetravalent solutes are more puzzling. Amorphous Fe-C data in Fig. 16 data^{61,62} have the wrong slope and such high values of moment at a given Z_m , compared to Fe-Si, for example, that it is difficult to attribute the deviations to clustering. Similarly, data^{47,55,63,64} on Fe-Ge in Fig. 17 lie high and scatter strongly. The data are complicated by the lack of good ferromagnetic saturation.⁶⁴ Data^{47,65} on Fe-Sn in Fig. 18 also lie high.

Finally, of the pentavalent solutes, Fe-As and Fe-Sb data⁴⁷ in Fig. 19 are restricted to too small a concentration range to reach our range of interest. Fe-P data^{53,58,66} show very high values for the crystals and lower values with the wrong slope for the amorphous phase. We presume that because of the highly attractive *sp* potential, states are being pulled through the gap and the theory no longer applies. For completeness, we also show Fe-Be

data⁴⁷ in Fig. 14 which seems to indicate a low value of $2N_{sp}^{\uparrow}$.

A summary of $2N_{sp}^{\uparrow}$ values is given in Table III for those cases where they can be extracted with confidence. More complete data are needed to draw convincing conclusions about the trends in these numbers, although (with the exception of Co-Au) our predicted tendency for $2N_{sp}^{\uparrow}$ to be lower for bcc than fcc alloys appears to hold.

We conclude that while the band-gap theory does not describe some systems and some details of the data, it does appear to be the correct starting point for most systems. This includes most Co and Fe alloys which have not been analyzed from this viewpoint before. We caution against an overly rigid interpretation of details such as the difference between bcc and fcc alloys and the transition between dilute and concentrated limits. More detailed experimental data or band calculations at other compositions will almost certainly reveal new systematics and hopefully explain some of the discrepancies. Nevertheless, we believe that the perspective developed in this paper provides the most coherent and justifiable framework for studying these systems, and we hope that it will encourage further such work.

ACKNOWLEDGMENTS

The authors thank K. Terakura for the valuable discussions which stimulated this work, and also R. C. O'Handley, B. Corb, W. Felsch, T. R. McGuire, R. J. Gambino, H. Claus, and many others for important input about the experimental data.

¹E. C. Stoner, *Philos. Mag.* **15**, 1018 (1933).

²N. F. Mott, *Proc. Phys. Soc. London* **47**, 571 (1935).

³K. Terakura and J. Kanamori, *Prog. Theor. Phys.* **46**, 1007 (1971).

⁴K. Terakura, *J. Phys. F* **6**, 1385 (1976); *Physica* **91B**, 162 (1977).

⁵N. F. Mott, *Adv. Phys.* **13**, 325 (1964).

⁶J. Friedel, *Nuovo Cimento* **10**, Suppl. No. 2, 287 (1958).

⁷A. P. Malozemoff, A. R. Williams, K. Terakura, V. L. Moruzzi, and K. Fukamichi, *J. Magn. Magn. Mater.* **35**, 192 (1983).

⁸A. R. Williams, V. L. Moruzzi, A. P. Malozemoff, and K.

Terakura, *IEEE Trans. Magn.* **MAG-19**, 1983 (1983).

⁹E. C. Stoner, *Proc. R. Soc. London* **169**, 339 (1939).

¹⁰O. Gunnarsson, *J. Phys. F* **6**, 587 (1976).

¹¹L. Berger, *Phys. Rev.* **137**, A220 (1965).

¹²J. C. Slater, *Phys. Rev.* **49**, 537 (1936).

¹³L. Pauling, *Phys. Rev.* **54**, 899 (1938).

¹⁴R. M. Bozorth, *Ferromagnetism* (Van Nostrand, New York, 1951).

¹⁵S. V. Vonsovski, *Magnetism* (Wiley, New York, 1974), p. 752.

¹⁶H. Ehrenreich and L. M. Schwartz, in *Solid State Physics*, edited by H. Ehrenreich, F. Seitz, and D. Turnbull (Academ-

- ic, New York, 1976), p. 149.
- ¹⁷R. Alben, J. I. Budnick, and G. S. Cargill III, in *Metallic Glasses* (American Society for Metals, Metal Park, Ohio, 1978), p. 304.
- ¹⁸J. Crangle and M. J. C. Martin, *Philos. Mag.* **4**, 1006 (1959); J. Crangle and D. Parsons, *Proc. R. Soc. London Ser. A* **255**, 509 (1960).
- ¹⁹N. Lundquist, H. P. Myers, and R. Westin, *Philos. Mag.* **7**, 1187 (1962).
- ²⁰J. Crangle, in *Electronic Structure and Alloy Chemistry of the Transition Elements*, edited by P. A. Beck (Wiley, New York, 1963), p. 51.
- ²¹K. Yamauchi and T. Mizoguchi, *J. Phys. Soc. Jpn.* **39**, 541 (1975).
- ²²F. E. Luborsky, in *Ferromagnetic Materials*, edited by E. P. Wohlfarth (North-Holland, Amsterdam, 1980), Vol. 1, p. 451.
- ²³R. C. O'Handley, in *Metallic Glasses*, edited by F. E. Luborsky (Butterworths, London, 1983), p. 257.
- ²⁴R. P. Messmer, *Phys. Rev. B* **23**, 1616 (1981).
- ²⁵B. W. Corb, R. C. O'Handley, and N. J. Grant, *Phys. Rev. B* **27**, 636 (1983).
- ²⁶K. W. H. Buschow and P. G. van Engen, *J. Appl. Phys.* **52**, 3557 (1981).
- ²⁷C. D. Gelatt, A. R. Williams, and V. L. Moruzzi, *Phys. Rev. B* **27**, 2005 (1983).
- ²⁸V. L. Moruzzi, J. F. Janak, and A. R. Williams, *Calculated Electronic Properties of Metals* (Pergamon, New York, 1978).
- ²⁹A. R. Williams, V. Moruzzi, C. D. Gelatt, Jr., J. Kübler, and K. Schwarz, *J. Appl. Phys.* **53**, 2019 (1982).
- ³⁰A. R. Williams, J. Kübler, and C. D. Gelatt, Jr., *Phys. Rev. B* **19**, 6094 (1979).
- ³¹T. Jo and H. Akai, *J. Phys. Soc. Jpn.* **50**, 70 (1981).
- ³²M. Takahashi, S. Ishio, and F. Sato, Supplement to Tohoku University Science Report No. 28, 1980, p. 287 (unpublished). Results quoted by Corb *et al.* (Ref. 25).
- ³³A. Barrada, M. F. Lapierre, B. Loegel, P. Panissod, and C. Robert, *J. Phys. F* **8**, 845 (1978).
- ³⁴A. W. Simpson and D. R. Brambley, *Phys. Status Solidi B* **43**, 291 (1971).
- ³⁵D. Pan and D. Turnbull, *J. Appl. Phys.* **45**, 1406 (1974).
- ³⁶T. Kanbe and K. Kanematsu, *J. Phys. Soc. Jpn.* **24**, 1396 (1958).
- ³⁷H. Watanabe, H. Morita, and H. Yamauchi, *IEEE Trans. Magn.* **14**, 944 (1978).
- ³⁸R. Hasegawa and R. Ray, *J. Appl. Phys.* **50**, 1586 (1979).
- ³⁹T. R. McGuire, J. A. Aboaf, and E. Klokhholm, *IEEE Trans. Magn.* **16**, 905 (1980). These data lie slightly lower than those of other workers (Refs. 37 and 38). We tentatively attribute this difference to systematic error in determining sample thickness.
- ⁴⁰W. Felsch, *Z. Angew. Phys.* **30**, 275 (1970).
- ⁴¹D. Parsons, W. Sucksmith, and J. E. Thompson, *Philos. Mag.* **3**, 1174 (1958). Data on Co-Si disagree with that of Felsch (Ref. 40). Since Parsons *et al.* did not directly determine alloy phase by x ray, and worked with the metastable fcc phase, we prefer Felsch's data and are similarly cautious about the Co-Al results.
- ⁴²G. Marchal, D. Teirlinck, P. Mangin, C. Janot, and J. Hubsch, *J. Phys. (Paris) Colloq.* **41**, C8-661 (1980).
- ⁴³T. R. McGuire, J. A. Aboaf, and E. Klokhholm, *J. Appl. Phys.* **53**, 8219 (1982).
- ⁴⁴T. R. McGuire, J. A. Aboaf, and E. Klokhholm, *J. Appl. Phys.* **52**, 2205 (1981).
- ⁴⁵S. Mader and A. S. Nowick, *Appl. Phys. Lett.* **7**, 57 (1965).
- ⁴⁶M. Fallot, *Ann. Phys. (Paris)* **6**, 305 (1936).
- ⁴⁷A. T. Aldred, *J. Phys. C* **1**, 1103 (1968).
- ⁴⁸A. Arrott and H. Sato, *Phys. Rev.* **114**, 1939 (1959); H. Sato and A. Arrott, *ibid.* **114**, 1427 (1959).
- ⁴⁹T. Wakiyama, *J. Phys. Soc. Jpn.* **32**, 1222 (1972).
- ⁵⁰H. Okamoto and P. A. Beck, *Monatsh. Chem.* **103**, 907 (1972).
- ⁵¹W. Felsch, *Z. Angew. Phys.* **29**, 217 (1970).
- ⁵²R. Hasegawa and R. Ray, *J. Appl. Phys.* **49**, 4174 (1978).
- ⁵³J. Durand and M. Yung, in *Amorphous Magnetism II*, edited by R. A. Levy and R. Hasegawa (Plenum, New York, 1977), p. 275.
- ⁵⁴H. Hiroyoshi, K. Fukamichi, M. Kikuchi, A. Hoshi, and T. Masumoto, *Phys. Lett.* **65A**, 163 (1978).
- ⁵⁵K. H. J. Buschow and P. G. van Engen, *J. Appl. Phys.* **52**, 3557 (1981).
- ⁵⁶T. R. McGuire, J. A. Aboaf, and E. Klokhholm, *IEEE Trans. Magn.* **16**, 905 (1980).
- ⁵⁷R. Ray and R. Hasegawa, *S. S. Commun.* **27**, 471 (1978).
- ⁵⁸M. C. Cadeville and E. J. Daniel, *J. Phys. (Paris)* **27**, 449 (1966).
- ⁵⁹M. Mitera, M. Naka, T. Masumoto, N. Kazama, and K. Watanabe, *Phys. Status Solidi A* **49**, K163 (1978).
- ⁶⁰P. Mangin and G. Marchal, *J. Appl. Phys.* **49**, 1709 (1978).
- ⁶¹N. Kazama and N. Heiman, *J. Appl. Phys.* **49**, 1706 (1978).
- ⁶²C. Guillaud, *C. R. Acad. Sci. (Paris)* **219**, 614 (1944).
- ⁶³P. Terzieff, K. Lee, and N. Heiman, *J. Appl. Phys.* **50**, 1031 (1979).
- ⁶⁴O. Massenot, *J. Phys. F* **9**, 1687 (1979).
- ⁶⁵P. Mangin, M. Piecuch, G. Marchal, and C. Janot, *J. Phys. F* **8**, 2085 (1978).
- ⁶⁶A. J. P. Meyer and M. C. Cadeville, *J. Phys. Soc. Jpn.* **17**, Suppl. B. 1, 223 (1962).